EGFR and EphA2 are hepatitis C virus host entry factors and targets for antiviral therapy

Joachim Lupberger, Mirjam B. Zeisel, Fei Xiao, Christine Thumann, Isabel Fofana, Laetitia Zona, Christopher Davis, Christopher J. Mee, Marine Turek, Sebastian Gorke, Cathy Royer, Benoit Fischer, Muhammad N. Zahid, Dimitri Lavillette, Judith Fresquet, François–Loïc Cosset, S. Michael Rothenberg, Thomas Pietschmann, Arvind H. Patel, Patrick Pessaux, Michel Doffoël, Wolfgang Raffelsberger, Olivier Poch, Jane A. McKeating, Laurent Brino and Thomas F. Baumert

SUPPLEMENTARY RESULTS AND DISCUSSION

RNAi screen identifies kinases with functional impact on HCV entry. To identify host cell kinases involved in HCV entry, we performed a small interfering RNA (siRNA)–based screen silencing 691 human kinases and associated proteins in Huh7 hepatoma cells to comprehensively identify cellular kinases regulating HCV entry. Screening comprised three steps: a primary screen using HCV pseudoparticles (HCVpp) bearing HCV envelope glycoproteins and vesicular stomatitis virus pseudotyped particles (VSVpp) as an unrelated control virus. To validate the relevance of the identified kinases in the complete infectious viral life cycle, identified hits were confirmed in a secondary screen using cell–culture–derived HCV (HCVcc) (**Supplementary Fig. 1**). False positive results due to toxicity were excluded using MTT–based cell viability test (**Supplementary Table 2**). To exclude non–specific off–target effects by siRNA pools, hits were validated using four individual siRNAs in a third screen (**Supplementary Fig. 1**). 106 kinases were identified by the primary HCVpp screen (**Supplementary Table 1**) and, of these, 95 were confirmed by infection with HCVcc. 58 of the 95 kinases passing the secondary screen were validated in the third screen (**Supplementary Table 2**).

The genome–wide RNAi kinase screen identified 58 kinases with impact on HCV entry and initiation of HCV infection (**Supplementary Table 2**). These kinases constituted 11.2% of the human kinome[1]. This percentage is in a similar range as previously published RNAi screens targeting human immunodeficiency virus (HIV) (4.3% of human kinome)[2] and West Nile Virus (6.4% of human kinome)[3]. Using a genome–wide RNAi screen, Li and co–workers identified 407 host genes required for HCVcc (JFH1) infection[4]. Among these hits were 14 kinases (2.7% of the human kinome); four of these kinases (29%) were confirmed in our screen. These kinases were CHKA, RYK, PTK2B and PI4KA. Thus, our screen identified 54 novel cellular kinases as host factors for HCV entry, including EGFR, EphA2, and CDC2, which had not been identified previously[4]. The relatively small overlap of hits in the two HCV RNAi screens is not unusual and has been observed for other RNAi screens identifying host factors for HIV infection[5]. Reasons include the use of different siRNA libraries (Qiagen vs. Dharmacon) and screening formats

(96 wells vs. 384 wells). Our screen was performed in a 96–well screening format with a particular focus on avoiding microplate edge effects, which increased the robustness and reproducibility (Z–value). This allowed us to use a more advanced statistical approach for threshold considerations with respect to significance analysis and false discovery rate considerations of each observed hit (see **Supplementary Methods**). In contrast to the genome–wide screen which was limited to a detailed bioinformatic analysis of the identified hits[4], our study for the first time provides a comprehensive functional analysis of kinases required predominantly for HCV entry by assessing the effect of gene silencing on HCVpp and VSVpp entry and HCVcc infection. Most importantly, we identified EGFR and EphA2 as novel co–factors for HCV entry, elucidated their functional relevance within the HCV entry process and identified them as targets for antiviral therapy.

Bioinformatic analyses identify kinase networks involved in HCV entry. For a classification of the known biological functions of the identified 58 kinases, we performed a bioinformatic analysis using the Ingenuity Pathways database[3]. This analysis revealed a high representation of genes involved in cell death (58.6%), amino acid metabolism, post–translational modification and small molecule biochemistry (51.7%), cancer (50.0%), cellular growth and proliferation (44.8%), and cell cycle as listed by percent frequency (**Supplementary Fig. 2a**). When classifying kinases with an impact on HCV but not VSV entry (**Supplementary Table 2**), amino acid metabolism, post–translational modification and small molecule biochemistry (19%), cell death (19%), cell morphology and development (15.5%), cellular function and maintenance (15.5%), cellular function and organization (13.8%), and cell signaling (12.1%), emerged among the top six categories as listed by percent frequency (**Supplementary Fig. 2b**).

Next, the identified hits were analyzed for known and predicted protein interactions using the STRING database[6]. STRING represents a meta–database mapping of all known protein–protein interactions onto a common set of genomes and proteins[6]. Analysis of the 58 kinases identified in the RNAi screen revealed kinase networks regulating cell morphology including cell polarity, tight junction (TJ) permeability, and cell adhesion, as well as networks of kinases involved in the cell cycle (**Supplementary Fig. 2c**). Key interactions were confirmed using the IntAct database[7]. However, STRING analysis resulted in the most detailed network, which is due to the fact that STRING contains the largest collection of data sets for protein–protein interactions. Furthermore, STRING provides detailed and integral quality–scores which are of great importance in keeping the rate of false positives as low as possible[6]. To further confirm the validity of the identified network, we randomly selected 1000 groups of 58 kinases (from a collective of 691 kinases and associated molecules) and compared the connectivity of these random collections to our identified network presented in **Supplementary Fig. 2**. The subsequent comparison revealed that none of the randomly chosen sets of 58 kinases shows a single instance ($P<0.001$) of our identified network or anything similar (matching at least 20% of the network in **Supplementary Fig. 2c**). Taken together, these results demonstrate that the network depicted in

Supplementary Fig. 2c is the result of extensive and reproducible bioinformatic analyses and highly distinct form a random product.

Five kinases are targets of clinically licensed protein kinase inhibitors (PKIs). These include ephrin receptor A2 EphA2 (*Dasatinib*), epidermal growth factor receptor EGFR (*Erlotinib*), cell division cycle 2 kinase CDC2 (*Flavopiridol*), cyclin–dependent kinase 4 CDK4 (*Flavopiridol*) and cyclin–dependent kinase 8 CDK8 (*Flavopiridol*) (**Supplementary Fig. 2c**). Silencing by kinase–specific siRNAs reduced HCVpp entry by 4.39 fold for EGFR, 3.05 fold for EphA2, 14.96 fold for CDC2, 9.76 fold for CDK4 and 6.36 fold for CDK8 (**Supplementary Table 2**).

Cell cycle control and HCV entry. STRING analysis pointed to a network that included 12 kinases involved in cell cycle regulation (**Supplementary Fig. 2c** and **Supplementary Table 2**), including CDC2, CDK4, CDK8, cholin kinase alpha (CHKA), cholin kinase beta (CHKB), cyclin–dependent kinase inhibitor 1B (CDKN1B), CDC28 protein kinase regulatory subunit 1B (CKS1B), ataxia telangiectasia mutated protein (ATM), polo–like kinase 1 (PLK1), polo–like kinase 3 (PLK3), aurora kinase B (AURKB), inhibitor of kappa light polypeptide gene enhancer kinase B in B–cells (IKBKB). Although we cannot exclude the possibility that these molecules were identified because of intrinsic properties of the cell division–dependent hepatoma model system, several observations support a specific role of cyclin–dependent kinases (CDKs) for HCV entry: first, silencing of kinases potently inhibited HCVpp entry and HCV infection (**Supplementary Table 2** and **Supplementary Fig. 12a–d**). Second, after gene silencing (apart from experiments with CHKA and IKBKB), no cytotoxicity was observed as measured by the cellular metabolite MTT (**Supplementary Table 2**). This suggests that the silencing of kinases was not due to non–specific toxic effects. Third, silencing/rescue experiments further confirmed a functional role for CDC2 in HCV entry (**Supplementary Fig. 12e**). Fourth, *Flavopiridol* — a well–characterized inhibitor of CDKs– markedly inhibited HCVpp entry in the absence of any detectable cytotoxic effects in PHH (**Supplementary Fig. 12f**). These data suggest that the effect of CDKs is not related to either the model target cell line or the pseudoparticle entry assay, and is relevant to HCV entry. It is well known that CDKs play an important role in the life cycle of HIV and herpes viruses. These include regulation of HIV transcription by CDK9[8] and the activation by Kaposi sarcoma–associated herpes virus of CDK4 and CDK6 that regulate microfilament organization and cell morphology[9]. Thus, it is conceivable that similar mechanisms apply for HCV entry.

Kinases involved in integrin signaling and HCV entry. Furthermore, the screen identified kinases involved in cell adhesion and integrin signaling: focal adhesion kinase (PTK2), focal adhesion kinase 2 (PTK2B), and integrin–linked kinase (ILK), all of these kinases regulate cell adhesion and cell–matrix interaction[10,11] (**Supplementary Table 2**). It has been shown that CD81 — a key HCV entry factor — and other tetraspanins are associated with adhesion receptors of the integrin family and regulate integrin–dependent cell migration[12]. It is thus conceivable that

functional integrin signaling might be a prerequisite for HCV entry factor trafficking and localization on the cell surface — and therefore for HCV entry. In this context a number of tetraspanins, including CD81, are associated with type II phosphatidylinositol 4–kinase and it is suggested that this may facilitate the assembly of signaling complexes by tethering these enzymes to integrin heterodimers[12]. It is of interest to note that silencing of phosphatidylinositol 4–kinase type 2 alpha (PI4KII) impaired HCV entry and infection (**Supplementary Table 1**). Moreover, it is known that integrin signaling plays a pivotal role in the entry of other viruses such as adenovirus, hantavirus and herpesviruses (for review see[13]): HCV may therefore have another integrin–dependent entry mechanism.

EGFR and EphA2 do not mediate HCV entry by modulation of cell polarity. EphA2 and EGFR are involved in regulation of cell polarity[14-17] and polarization has been shown to restrict HCV entry[18,19]. Since blocking kinase function inhibited HCV entry, we investigated whether PKI treatment modulated HepG2 polarization. *Dasatinib* reduced HepG2 polarization and *Erlotinib* had no effect (**Supplementary Fig. 9a**). TJ integrity was not affected (**Supplementary Fig. 9b**). These data indicate that the marked inhibition of HCV entry cannot be explained by a PKI–induced decrease in polarization.

Modulation of HCV entry by EphA2–specific ligands and antibodies. Since EphA2 is constitutively active and its degradation is modulated by membrane–bound ligands during cell–cell contact[20-22], the investigation of ligand–induced activation of EphA2 in cell culture models is technically more complex. To address this question, we used soluble model ligands ephrin–A1 and –A3 which have been reported to mimic some but not all mechanisms of cell–cell contact[21]. Ephrin–A1 and –A3 have been shown to induce the degradation of cell surface EphA2[20,21]. The addition of ephrin–A1 or –A3 but not of control ligand resulted in a small but highly reproducible and significant (P<0.0005) decrease of HCV entry that was dependent on target cell density (**Supplementary Fig. 6a**). To further address the role of EphA2 ligand binding domain for HCV entry, we produced polyclonal antibodies to the EphA2 extracellular loop by genetic immunization. The polyclonal antibodies specifically bound to the native EphA2 extracellular domain as demonstrated by the specific binding of the antibodies to non–permeabilized BOSC and CHO cells transfected to express human EphA2 (**Supplementary Fig. 6b** and data not shown) and the HCV permissive hepatoma cell line Huh7.5.1 (**Supplementary Fig. 6c**). Pre–incubation of PHH with antibodies to EphA2 significantly (P<0.005) inhibited HCV entry, suggesting that engagement of the EphA2 extracellular domain contributes to its effect on HCV entry (**Supplementary Fig. 6d**).

Clinical approved PKIs inhibit entry of highly diverse HCV escape variants. *Erlotinib* and *Dasatinib* inhibited HCV infection at dose ranges (IC_{50} 0.45–0.53 μM) similar to mean plasma concentrations of patients during cancer treatment (*Dasatinib* ~0.2 μM; *Erlotinib* ~4 μM)[23-25]. Furthermore, *Flavopiridol* inhibited HCV entry (IC_{50} 0.005 μM) in concentrations well below

clinical use in cancer treatment (~2 μM[26]) (**Supplementary Fig. 12f**). Therefore, we further assessed the potential of PKIs as antivirals by investigating their impact on infection of 14 HCV strains isolated from 6 patients undergoing liver transplantation[27]. These variants re–infecting the liver graft ("escape variants") were characterized by high infectivity and marked resistance to autologous host neutralizing responses[27]. Pre–incubation of cells with approved kinase inhibitors markedly and significantly (P<0.0005) inhibited entry of HCV escape variants in PHH and Huh7.5.1 cells without decreasing cell viability (**Supplementary Fig. 11**, data not shown). In contrast, pre–incubation of cells with *Blebbistatin*, an unrelated small molecule inhibitor did not decrease entry of HCV isolates (**Supplementary Fig. 11**). These data demonstrate that *Erlotinib*, *Dasatinib* and *Flavopiridol* inhibit entry of highly infectious HCV escape variants, which are resistant to autologous neutralizing antibodies.

Clinical implications of identified RTKs for HCV pathogenesis and treatment. *In vivo*, expression of EphA2 and EGFR has been shown to be elevated in HCV–induced hepatocellular carcinoma (HCC)[28,29]. However, a detailed analysis of EGFR and EphA2 expression in the hepatocytes of HCV–infected patients *in vivo* is not yet available. TGF–α expression is elevated in the liver of HCC or chronically HCV infected patients[30]. In *in vitro* model systems, EGFR expression is increased in HCV infected cells[31]. Furthermore, HCV non–structural protein NS5A has been reported to alter EGFR trafficking[32] and HCV NS3/4A protease activates EGFR–induced signal transduction[33]. HCV core protein has been reported to enhance expression of TGF–α – an EGFR ligand[34]. Finally, HCV NS4B has been shown to enhance EphA2 expression[35]. Taken together, these findings suggest that HCV may not only use RTKs as co–factors for HCV entry but at the same time modulates their expression and function. Further studies are underway to investigate the relevance of virus–induced regulation of EGFR expression and signaling for HCV entry and pathogenesis of HCV infection (e.g. the presence of virus–induced positive feedback loops).

Furthermore, our results have important clinical implications for the prevention and treatment of HCV infection. PKIs and antibodies to RTKs are well established and approved drugs for cancer treatment and have a well characterized and manageable safety profile in humans[36,37]. Similar to standard of care or direct acting antivirals (DAAs) in development, the clinical use of these inhibitors is limited by adverse effects. Next generation EGFR kinase inhibitors with improved safety profiles[38] may address this limitation and thus are interesting antiviral candidates in the future. Although the antiviral potency of PKIs appears to be lower than DAAs targeting viral protein processing and replication, PKIs and monoclonal antibodies to RTKs are very attractive and clinically relevant antiviral compounds since they target complementary host factors required for viral infection. Indeed, there is increasing evidence that targeting essential host factors will increase the genetic barrier for viral resistance[39-41] and that ultimately a combination of complementary antivirals will be required to prevent antiviral resistance[41]. This concept is further supported by our results demonstrating that PKIs efficiently inhibit entry of escape viruses that are resistant to patients' immune responses (**Supplementary**

Fig. 11). Thus, the development of PKIs specifically targeting the proviral function of RTKs and the combination of PKIs with DAAs or standard of care may further increase their antiviral activity in eradicating HCV. Finally, a case report describing HCV clearance during *Erlotinib* treatment of a patient with metastatic hepatocellular carcinoma and chronic HCV infection provides further clinical evidence for an antiviral effect of PKIs *in vivo*[42].

SUPPLEMENTARY METHODS

Genome–wide RNAi kinase HCV entry screen. Screening was performed at the High Throughput Screening platform of the Institut de Génétique et de Biologie Moléculaire et Cellulaire (IGBMC) in Illkirch, France. The library used for this screen was the Human Kinase siRNA Set Version 2.0 (pool of four siRNAs) and individual siRNAs were obtained from Qiagen. A functional HCV entry siRNA screen targeting 691 cellular kinases and associated proteins was established as outlined (**Supplementary Fig. 1**). For each target 3.5 pmol siRNA was reverse transfected in 5,000 Huh7 cells 0.3 cm^{-2} using INTERFERin reagent (Polyplus). The effect of gene silencing on viral entry was investigated three days after siRNA transfection using HCVpp (H77; genotype 1a)[27,43] harboring a luciferase reporter gene. Impact on VSVpp entry was analyzed side–by–side. Virus entry was assessed two days after infection by measuring reporter gene luciferase activity in cell lysates using the Bright Glo Luciferase assay system (Promega) and a Mithras LB 940 luminometer (Berthold Technologies). Hits were validated independently using four different single siRNAs silencing the same target mRNA. Validation using HCVcc strain Luc–Jc1[44] ($TCID_{50}$ 10^3 mL^{-1}–10^4 mL^{-1}) was performed in Huh7.5.1 cells using the same protocol as described above. All siRNA screens were performed in 96–well cell culture microplates. Luciferase results were normalized by protein content of the lysates using DC Protein Assay (Bio–Rad). To minimize non–specific effects due to evaporation, outside wells were not used for the screens but were filled with phosphate buffered saline (PBS). Non–specific effects of gene silencing due to changes in cell proliferation were normalized by measuring the protein content of the individual well. The quality of the established high–throughput screens, the individual plate designs as well as the amount of replicates were assessed in pilot experiments by calculating the Z–factor[45]. The HCVpp screens (Z=0.37) were performed in duplicates with 60 of 96 central plate positions used for the screen. The HCVcc validation screens (Z=0.47) were performed in triplicates with 32 of 96 central plate positions used for the screen. As an internal quality control of gene silencing and HCVpp and HCVcc infection, positive and negative control siRNAs (targeting CD81 and GFP, respectively) were transfected side–by–side on each plate. Cytotoxic effects on cells were assessed in triplicates by analyzing the ability to metabolize 3–(4,5–dimethylthiazol–2–yl)–2,5–diphenyltetrazolium bromide (MTT) as described (**Methods**).

Statistical analysis: hit selection. The impact of gene silencing was defined by an increase or decrease of HCVpp entry expressed as the ratio of entry compared to the experimental mean value of entry into control transfected cells (siRNA targeting GFP). The local false discovery rates (fdr) for all comparisons for each gene were determined using the library "fdrtool"[46]. Resulting fdr–value were examined for their distribution in order to define meaningful cut–offs (data not shown). Finally, for HCVpp a threshold of fdr<0.001 (corresponding to a maximum p–value of 1.04×10^{-4}), for HCVcc a threshold of fdr<0.05 (corresponding to a maximum p–value of 2.05×10^{-2}) and for VSVpp a threshold of fdr<0.08 (corresponding to a maximum p–value of 8.03×10^{-2}) were chosen as stringent parameters based on the underlying frequency distributions

(data not shown). All candidates chosen for further validation are highlighted in **Supplementary Table 1**. To address potential off–target effects by pooled siRNAs, candidate genes were validated if HCV entry was reduced ≥50% compared to control transfected cells by at least two individual siRNAs (**Supplementary Table 2**).

Gene ontology and gene annotation. Gene ontology terms and gene associations were obtained from Human Kinase siRNA Set Version 2.0 validated by Ingenuity Pathways database (Mountainview, CA, USA). Biological function analysis of the identified kinases was performed using Ingenuity Pathways database[3]. Biological function terms were accepted if they were significantly enriched with a p–value $<10^{-5}$ as calculated by Ingenuity Pathways database. Additionally, the identified hits were analyzed for known and predicted protein interactions using STRING meta–database that maps all interaction evidence onto a common set of genomes and proteins[6]. The interactions addressed include direct (physical) and indirect (functional) associations derived from numerous sources, including experimental repositories, computational prediction methods and public text collections[6].

HCV strains for production of HCVpp and HCVcc. HCVpp from strains H77, HCV–J, JFH1, J6, UKN2A.2.4, UKN3A1.28, UKN4.21.16, P01VL, P02VH, P02VI, P02VJ, P03VC, P04VC, P04VD, P04VE, P05VD, P05VE, P05VF, P06VG, P06VH, P06VI[27,43,47] and HCVcc[44,48] (strains JFH1, Jc1, Luc–Jc1) were produced as described.

siRNAs and expression plasmids used for rescue experiments and functional studies. siEGFR si3 (Hs–EGFR_6, 5'–CAUCCAAUUUAUCAAGGAATT–3') and si4 (Hs–EGFR_12, 5'–GGAACUGGAUAUUCUGAAATT–3'), siEphA2 si4 (Hs–EPHA2_8, 5'–GGACAGACAU AUAGGAUAUTT–3'), siCDC2 (Hs–CDC2_14, 5'–GGUUAUAUCUCAUCUUUGATT–3') were obtained from Qiagen. siCTRL, siCD81, siSR–BI have been described[48]. Lentiviral expression plasmids pLKO–shEGFR[49], pWPI–EGFRWT[49], pEGFR–L858R[50], and expression plasmid pEphA2–WT[51] and pCDC2–WT (Addgene plasmid 1886)[52] have been described.

Protein kinase inhibitors, ligands and antibodies. *Erlotinib*, *Gefitinib*, *Lapatinib* and *Dasatinib* were obtained from IC Laboratories, *Flavopiridol* and Concanamycin A from Sigma, BILN–2061 from Boehringer Ingelheim and IFN–α–2a from Roche. All other small molecules and DMSO (used at a final concentration 0.7% for incubation of PKIs and control experiments) were obtained from Merck. Recombinant EGF and TGF–α were obtained from Sigma and soluble tagged ephrin ligands and tag controls from R&D. Production and purification of soluble His–tagged HCV E2 glycoprotein has been described[53]. Antibodies to EGFR (528), CD81 (5A6), EphA2 (C–20), and occludin (H–279) were obtained from Santa Cruz; antibody to E2 (AP33) from Genentech, antibody to EGFR (LA–1) from Millipore; antibody to NS5A from Virostat; antibody to CD81 (JS81) from BD; antibody to CLDN1 (1C5–D9) from Abnova; antibody to occludin (OC–3F10) from Zymed; antibody to actin (EP1123Y) from Abcam; antibody to CDC2 from Cell Signaling; antibody to His_5 from Qiagen, PE–conjugated antibody to mouse and Cy3–

conjugated antibody to mouse from Jackson ImmunoResearch, alkaline–phosphatase (AP)–labeled secondary antibodies from GE Healthcare. Polyclonal antibody to human EphA2 was raised by genetic immunization of Wistar rats by an expression vector containing the full–length human EphA2 cDNA as described previously for CLDN1-specific antibodies[54]. Polyclonal SR–BI–specific antibodies used for E2binding and postbinding experiments has been described[48,55].

Cell lines and primary hepatocytes. The sources and culture conditions for BOSC, CHO, 293T, Huh7, Huh7.5, Huh7.5.1 and HepG2–CD81 cells have been described[19,43,56,57]. Primary human hepatocytes (PHH) were isolated and cultured as described[54]. The mouse hepatoma cell line AML12 (#CRL–2254) was obtained from ATCC. The AML12 4R cell line was created by lentiviral gene transfer using lentiviruses transducing individual human CD81, SR–BI, CLDN1 and OCLN genes and subsequent selection of transduced cells with blasticidin and G418 as described previously[58]. The AML12 4R–hEGFR+ cell line was created by lentiviral gene transfer using vector pEGFR–L858R transducing active human EGFR[50].

HCV infection of primary hepatocytes. One day following PHH isolation and plating, PHH were washed with PBS and pre–incubated in the presence or absence of EGF, TGF–α, PKIs, EGFR–specific antibody or EphA2–specific serum for 1 h at 37 °C in William's E medium. Then, HIV–based HCVpp (J6)[54], HCVcc (J6–JFH1; Jc1, genotype 2a/2a, $TCID_{50}$: 10^5 mL^{-1}–10^6 mL^{-1})[59] or serum–derived HCV (HCV–positive infectious serum, genotype 1b described in ref.[40]) were added for 4 h at 37 °C. Following infection, fresh medium was added. HCVpp entry was assessed by measurement of luciferase activity 72 h postinfection as described[27,54]. HCVcc and infection with serum–derived HCV were assessed by HCV–specific qRT–PCR of purified intracellular HCV RNA as described[40].

Analyses of mRNA and protein expression. Cellular mRNA was extracted using RNeasy extraction kit (Qiagen) and quantified by qRT–PCR using Fastlane Cell Sybr Green kit (Qiagen)[48]. Western blots of cell lysates using protein–specific antibodies was performed following GE Healthcare protocols using Hybond–P membranes and visualized using ECF substrate and Typhoon Trio high performance fluorescence scanner (GE Healthcare). Immunostaining of HCV–infected cells was performed as described[60]. Kinase expression in liver was further confirmed by GeneAtlas database (BioGPS, Novartis Research Foundation, http://biogps.gnf.org) and is indicated (**Supplementary Table 2**).

Analysis of IC_{50} for PKIs and EGFR–specific antibody. IC_{50} was derived by logistic regression[61] using OriginPro (OriginLabs). IC_{50} values are expressed as median of three independent experiments ± standard error of the median.

Analysis of HCV postbinding steps and entry kinetics. HCV postbinding steps and entry kinetics were investigated as described[48,54]. Briefly, HCVcc (Luc–Jc1; genotype 2a/2a) binding to

Huh7.5.1 cells or HCVpp (P01VL, genotype 1b) binding to PHH was performed for 1 h at 4 °C in the presence or absence of heparin (250 μg mL^{-1}), control or anti–CD81 (5 and 10 μg mL^{-1}) and anti–EGFR IgG (10 and 50 μg mL^{-1}), anti–SR–BI or control serum (1:50), DMSO (0.7%) or PKIs (10 μM), Concanamycin A (ConA, 25 nM), before cells were washed and incubated with the indicated compounds for 4 h at 37 °C. HCVcc infection and HCVpp entry were assessed by luciferase reporter gene assay and expressed relative to control infections without addition of inhibitors as described[48,54,62,63]. For the study of HCV entry kinetics, compounds were added every 20 min for up to 120 min after viral binding. To assess the effect of EGF on HCVcc entry kinetics, serum–starved Huh7.5.1 cells were pre–incubated in serum–free medium in the presence or absence of EGF (1 μg mL^{-1}) prior to HCVcc binding and entry in the presence or absence of EGF (1 μg mL^{-1}). Complete medium supplemented with EGF (1 μg mL^{-1}) was added after the 4 h incubation period at 37 °C for 48 h.

SUPPLEMENTARY REFERENCES

1. Manning, G., Whyte, D.B., Martinez, R., Hunter, T. & Sudarsanam, S. The protein kinase complement of the human genome. *Science* **298**, 1912-1934 (2002).
2. Brass, A.L., *et al.* Identification of host proteins required for HIV infection through a functional genomic screen. *Science* **319**, 921-926 (2008).
3. Krishnan, M.N., *et al.* RNA interference screen for human genes associated with West Nile virus infection. *Nature* **455**, 242-245 (2008).
4. Li, Q., *et al.* A genome-wide genetic screen for host factors required for hepatitis C virus propagation. *Proc. Natl. Acad. Sci. U. S. A.* **106**, 16410-16415 (2009).
5. Kok, K.H., Lei, T. & Jin, D.Y. siRNA and shRNA screens advance key understanding of host factors required for HIV-1 replication. *Retrovirology* **6**, 78 (2009).
6. Jensen, L.J., *et al.* STRING 8--a global view on proteins and their functional interactions in 630 organisms. *Nucleic Acids Res.* **37**, D412-416 (2009).
7. Aranda, B., *et al.* The IntAct molecular interaction database in 2010. *Nucleic. Acids Res.* **38**, D525-531 (2010).
8. Zhou, M., *et al.* Bromodomain protein Brd4 regulates human immunodeficiency virus transcription through phosphorylation of CDK9 at threonine 29. *J. Virol.* **83**, 1036-1044 (2009).
9. Cuomo, M.E., *et al.* Regulation of microfilament organization by Kaposi sarcoma-associated herpes virus-cyclin.CDK6 phosphorylation of caldesmon. *J. Biol. Chem.* **280**, 35844-35858 (2005).
10. De Nichilo, M.O., Katz, B.Z., O'Connell, B. & Yamada, K.M. De novo expression of pp125FAK in human macrophages regulates CSK distribution and MAP kinase activation but does not affect focal contact structure. *J. Cell. Physiol.* **178**, 164-172 (1999).
11. Harburger, D.S. & Calderwood, D.A. Integrin signalling at a glance. *J. Cell. Sci.* **122**, 159-163 (2009).
12. Berditchevski, F. Complexes of tetraspanins with integrins: more than meets the eye. *J. Cell. Sci.* **114**, 4143-4151 (2001).
13. Stewart, P.L. & Nemerow, G.R. Cell integrins: commonly used receptors for diverse viral pathogens. *Trends Microbiol.* **15**, 500-507 (2007).
14. Basuroy, S., Seth, A., Elias, B., Naren, A.P. & Rao, R. MAPK interacts with occludin and mediates EGF-induced prevention of tight junction disruption by hydrogen peroxide. *Biochem. J.* **393**, 69-77 (2006).
15. Lackmann, M. & Boyd, A.W. Eph, a protein family coming of age: more confusion, insight, or complexity? *Sci. Signal.* **1**, re2 (2008).
16. Singh, A.B. & Harris, R.C. Epidermal growth factor receptor activation differentially regulates claudin expression and enhances transepithelial resistance in Madin-Darby canine kidney cells. *J. Biol. Chem.* **279**, 3543-3552 (2004).

17. Tanaka, M., Kamata, R. & Sakai, R. EphA2 phosphorylates the cytoplasmic tail of Claudin-4 and mediates paracellular permeability. *J. Biol. Chem.* **280**, 42375-42382 (2005).
18. Mee, C.J.*, et al.* Effect of cell polarization on hepatitis C virus entry. *J. Virol.* **82**, 461-470 (2008).
19. Mee, C.J.*, et al.* Polarization restricts hepatitis C virus entry into HepG2 hepatoma cells. *J. Virol.* **83**, 6211-6221 (2009).
20. Binns, K.L., Taylor, P.P., Sicheri, F., Pawson, T. & Holland, S.J. Phosphorylation of tyrosine residues in the kinase domain and juxtamembrane region regulates the biological and catalytic activities of Eph receptors. *Mol. Cell Biol.* **20**, 4791-4805 (2000).
21. Walker-Daniels, J., Riese, D.J., 2nd & Kinch, M.S. c-Cbl-dependent EphA2 protein degradation is induced by ligand binding. *Mol. Cancer Res.* **1**, 79-87 (2002).
22. Himanen, J.P.*, et al.* Architecture of Eph receptor clusters. *Proc. Natl. Acad. Sci. U. S. A.* **107**, 10860-10865 (2010).
23. Christopher, L.J.*, et al.* Metabolism and disposition of dasatinib after oral administration to humans. *Drug Metab. Dispos.* **36**, 1357-1364 (2008).
24. Frohna, P.*, et al.* Evaluation of the absolute oral bioavailability and bioequivalence of erlotinib, an inhibitor of the epidermal growth factor receptor tyrosine kinase, in a randomized, crossover study in healthy subjects. *J. Clin. Pharmacol.* **46**, 282-290 (2006).
25. Prados, M.D.*, et al.* Phase 1 study of erlotinib HCl alone and combined with temozolomide in patients with stable or recurrent malignant glioma. *Neuro. Oncol.* **8**, 67-78 (2006).
26. Byrd, J.C.*, et al.* Flavopiridol administered using a pharmacologically derived schedule is associated with marked clinical efficacy in refractory, genetically high-risk chronic lymphocytic leukemia. *Blood* **109**, 399-404 (2007).
27. Fafi-Kremer, S.*, et al.* Viral entry and escape from antibody-mediated neutralization influence hepatitis C virus reinfection in liver transplantation. *J. Exp. Med.* **207**, 2019-2031 (2010).
28. Yang, P.*, et al.* Overexpression of EphA2, MMP-9, and MVD-CD34 in hepatocellular carcinoma: Implications for tumor progression and prognosis. *Hepatol. Res.* **39**, 1169-1177 (2009).
29. Buckley, A.F., Burgart, L.J., Sahai, V. & Kakar, S. Epidermal growth factor receptor expression and gene copy number in conventional hepatocellular carcinoma. *Am. J. Clin. Pathol.* **129**, 245-251 (2008).
30. Chung, Y.H.*, et al.* Expression of transforming growth factor-alpha mRNA in livers of patients with chronic viral hepatitis and hepatocellular carcinoma. *Cancer* **89**, 977-982 (2000).
31. Duong, F.H., Christen, V., Lin, S. & Heim, M.H. Hepatitis C virus-induced up-regulation of protein phosphatase 2A inhibits histone modification and DNA damage repair. *Hepatology* **51**, 741-751 (2010).

32. Mankouri, J., Griffin, S. & Harris, M. The hepatitis C virus non-structural protein NS5A alters the trafficking profile of the epidermal growth factor receptor. *Traffic* **9**, 1497-1509 (2008).
33. Brenndorfer, E.D., *et al.* Nonstructural 3/4A protease of hepatitis C virus activates epithelial growth factor-induced signal transduction by cleavage of the T-cell protein tyrosine phosphatase. *Hepatology* **49**, 1810-1820 (2009).
34. Sato, Y., *et al.* Hepatitis C virus core protein promotes proliferation of human hepatoma cells through enhancement of transforming growth factor alpha expression via activation of nuclear factor-kappaB. *Gut* **55**, 1801-1808 (2006).
35. Zheng, Y., *et al.* Gene expression profiles of HeLa Cells impacted by hepatitis C virus non-structural protein NS4B. *J. Biochem. Mol. Biol.* **38**, 151-160 (2005).
36. Shepherd, F.A., *et al.* Erlotinib in previously treated non-small-cell lung cancer. *N. Engl. J. Med.* **353**, 123-132 (2005).
37. Wong, S.F. Dasatinib dosing strategies in Philadelphia chromosome-positive leukemia. *J. Oncol. Pharm. Pract.* **15**, 17-27 (2009).
38. Pao, W. & Chmielecki, J. Rational, biologically based treatment of EGFR-mutant non-small-cell lung cancer. *Nat. Rev. Cancer* **10**, 760-774 (2010).
39. Lanford, R.E., *et al.* Therapeutic silencing of microRNA-122 in primates with chronic hepatitis C virus infection. *Science* **327**, 198-201 (2010).
40. Fofana, I., *et al.* Monoclonal anti-claudin 1 antibodies prevent hepatitis C virus infection of primary human hepatocytes. *Gastroenterology* **139**, 953-964, 964 e951-954 (2010).
41. Georgel, P., *et al.* Virus-host interactions in hepatitis C virus infection: implications for molecular pathogenesis and antiviral strategies. *Trends Mol. Med.* **16**, 277-286 (2010).
42. Bardou-Jacquet, E., Lorho, R. & Guyader, D. Kinase inhibitors in the treatment of chronic hepatitis C virus. *Gut*, in press (2010).
43. Bartosch, B., Dubuisson, J. & Cosset, F.L. Infectious hepatitis C virus pseudo-particles containing functional E1-E2 envelope protein complexes. *J. Exp. Med.* **197**, 633-642 (2003).
44. Pietschmann, T., *et al.* Construction and characterization of infectious intragenotypic and intergenotypic hepatitis C virus chimeras. *Proc. Natl. Acad. Sci. U. S. A.* **103**, 7408-7413 (2006).
45. Zhang, J.H., Chung, T.D. & Oldenburg, K.R. A simple statistical parameter for use in evaluation and validation of high throughput screening assays. *J. Biomol. Screen.* **4**, 67-73 (1999).
46. Strimmer, K. fdrtool: a versatile R package for estimating local and tail area-based false discovery rates. *Bioinformatics* **24**, 1461-1462 (2008).
47. Lavillette, D., *et al.* Characterization of host-range and cell entry properties of the major genotypes and subtypes of hepatitis C virus. *Hepatology* **41**, 265-274 (2005).

48. Zeisel, M.B., *et al.* Scavenger receptor class B type I is a key host factor for hepatitis C virus infection required for an entry step closely linked to CD81. *Hepatology* **46**, 1722-1731 (2007).
49. Rothenberg, S.M., *et al.* Modeling oncogene addiction using RNA interference. *Proc. Natl. Acad. Sci. U. S. A.* **105**, 12480-12484 (2008).
50. Li, J., *et al.* A chemical and phosphoproteomic characterization of dasatinib action in lung cancer. *Nat. Chem. Biol.* **6**, 291-299 (2010).
51. Wang, Y., *et al.* Negative regulation of EphA2 receptor by Cbl. *Biochem. Biophys. Res. Commun.* **296**, 214-220 (2002).
52. van den Heuvel, S. & Harlow, E. Distinct roles for cyclin-dependent kinases in cell cycle control. *Science* **262**, 2050-2054 (1993).
53. Dreux, M., *et al.* Receptor complementation and mutagenesis reveal SR-BI as an essential HCV entry factor and functionally imply its intra- and extra-cellular domains. *PLoS Pathog.* **5**, e1000310 (2009).
54. Krieger, S.E., *et al.* Inhibition of hepatitis C virus infection by anti-claudin-1 antibodies is mediated by neutralization of E2-CD81-claudin-1 associations. *Hepatology* **51**, 1144-1157 (2010).
55. Kapadia, S.B., Barth, H., Baumert, T., McKeating, J.A. & Chisari, F.V. Initiation of hepatitis C virus infection is dependent on cholesterol and cooperativity between CD81 and scavenger receptor B type I. *J. Virol.* **81**, 374-383 (2007).
56. Zhong, J., *et al.* Robust hepatitis C virus infection in vitro. *Proc. Natl. Acad. Sci. U. S. A.* **102**, 9294-9299 (2005).
57. Lindenbach, B.D., *et al.* Complete replication of hepatitis C virus in cell culture. *Science* **309**, 623-626 (2005).
58. Haid, S., Windisch, M.P., Bartenschlager, R. & Pietschmann, T. Mouse-specific residues of claudin-1 limit hepatitis C virus genotype 2a infection in a human hepatocyte cell line. *J. Virol.* **84**, 964-975 (2010).
59. Ciesek, S., *et al.* Glucocorticosteroids increase cell entry by hepatitis C virus. *Gastroenterology* **138**, 1875-1884 (2010).
60. Barth, H., *et al.* Scavenger receptor class B is required for hepatitis C virus uptake and cross-presentation by human dendritic cells. *J. Virol.* **82**, 3466-3479 (2008).
61. Casato, M., *et al.* Predictors of long-term response to high-dose interferon therapy in type II cryoglobulinemia associated with hepatitis C virus infection. *Blood* **90**, 3865-3873 (1997).
62. Haberstroh, A., *et al.* Neutralizing host responses in hepatitis C virus infection target viral entry at postbinding steps and membrane fusion. *Gastroenterology* **135**, 1719-1728 e1711 (2008).
63. Koutsoudakis, G., *et al.* Characterization of the early steps of hepatitis C virus infection by using luciferase reporter viruses. *J. Virol.* **80**, 5308-5320 (2006).

64. Miura, K., Nam, J.M., Kojima, C., Mochizuki, N. & Sabe, H. EphA2 engages Git1 to suppress Arf6 activity modulating epithelial cell-cell contacts. *Mol. Biol. Cell* **20**, 1949-1959 (2009).
65. Pestka, J.M., *et al.* Rapid induction of virus-neutralizing antibodies and viral clearance in a single-source outbreak of hepatitis C. *Proc. Natl. Acad. Sci. U. S. A.* **104**, 6025-6030 (2007).

SUPPLEMENTARY TABLE LEGENDS

The contents of **Supplementary Tables 1** and **2** are provided as datasets in the online supplementary information.

Supplementary Table 1. Effect of silencing of 691 cellular kinases and associated proteins on HCVpp and VSVpp entry (primary screen). Using the Human Kinase RNAi Set Version 2.0 (pool of four siRNAs, Qiagen) and the Huh7–HCVpp system as a high–throughput model system for HCV entry we determined the impact of kinase gene silencing on entry of HCVpp (H77; genotype 1a) and VSVpp. Results are expressed as fold change of particle entry caused by gene silencing compared to particle entry into control siRNA–transfected cells (fold change = –1/fold infection, if the entry was reduced after kinase silencing; e.g. 50% decreased particle entry equals a fold infection of 0.5 and fold change of –2; e.g. 50% increased particle entry equals a fold infection of 1.5 and fold change of 1.5). Local false discovery rates (fdr) for each gene were determined using fdr analysis. Fdr threshold for hit selection (HCVpp entry) was <0.001, fdr threshold for HCV specificity (VSVpp entry) was <0.08. We identified a panel of 106 cellular kinases chosen for further validation (highlighted in yellow). Silencing of 42 kinases only decreased HCVpp infection (column J "HCV") but did not inhibit entry of VSVpp. Silencing of 64 kinases inhibited both HCVpp and VSVpp entry (column J "HCV+VSV"). For verification, we re–analyzed the screening results using ≥2 SDs from the plate mean as measure of threshold for hit selection (average measure) (the analysis strategy used by Brass et al.[2]). Using this method at least the same kinases would have been identified for subsequent validation screening (column K).

Supplementary Table 2. Cellular kinases modulating HCV entry identified by the RNAi kinase screen. Using the Human Kinase RNAi Set Version 2.0 (Qiagen), four individual siRNAs per target, we determined the impact of gene silencing on HCVpp, VSVpp and HCVcc infection and on cell viability (MTT). Results are expressed as fold change of pseudoparticle entry in cells with silenced kinase expression compared to control siRNA–transfected cells (fold change = –1/fold infection, if the entry was reduced after kinase silencing; e. g. 50% decreased particle entry equals a fold infection of 0.5 and fold change of –2; e. g. 50% increased particle entry equals a fold infection of 1.5 and fold change of 1.5). Local false discovery rates (fdr) and p–values for each gene were determined using fdr analysis. Following statistical analysis of the results from the primary and secondary screens and validation with individual siRNAs, we identified a panel of 58 cellular kinases exhibiting a significant (**Supplementary Methods**) impact on HCV entry and HCVcc infection that were validated by at least 2 of four individual siRNA. 18 kinases had an impact on HCV entry but not on entry of VSV (highlighted in blue). Kinase expression in liver was confirmed by GeneAtlas database (BioGPS, Novartis Research Foundation, http://biogps.gnf.org) and indicated in column N: relative gene expression is + = lower, ++ =

higher, +++ = 3 fold higher, ++++ = 10 fold higher than the median expression in all investigated tissues (>60).

SUPPLEMENTARY FIGURES

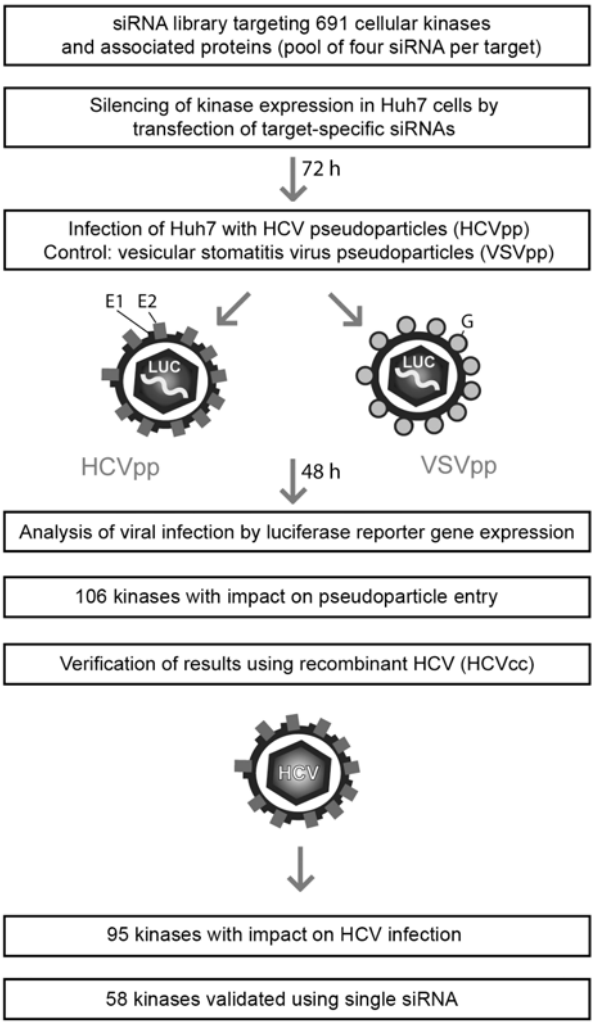

Supplementary Fig. 1. Schematic outline of the functional RNAi HCVpp entry screen used to identify HCV entry factors. Protein kinase expression was silenced in Huh7 hepatoma cells by target–specific siRNAs. Retroviral HCV pseudotyped particles (HCVpp) bearing HCV envelope glycoproteins (E1, E2) on their viral surface and harboring a luciferase reporter gene were used to analyze the impact of gene silencing on HCV entry into Huh7 cells. A decrease or increase in luciferase expression compared to the control siRNA–transfected cells indicated modulation of HCVpp entry by the corresponding target gene or genes. The effects of gene silencing on the infection of vesicular stomatitis virus derived pseudoparticles (VSVpp) were studied in side–by–side experiments. A RNAi library consisting of 691 siRNA pools was used to screen for cellular kinases and associated proteins with impact on entry of HCVpp. 106 candidates were identified in the primary RNAi screen. Pertinence to the infectious viral life cycle was verified for 95 candidate genes using recombinant HCVcc. 58 cellular kinases were validated by at least 2 individual siRNAs, thereby minimizing false positive hit selection due to off–target effects.

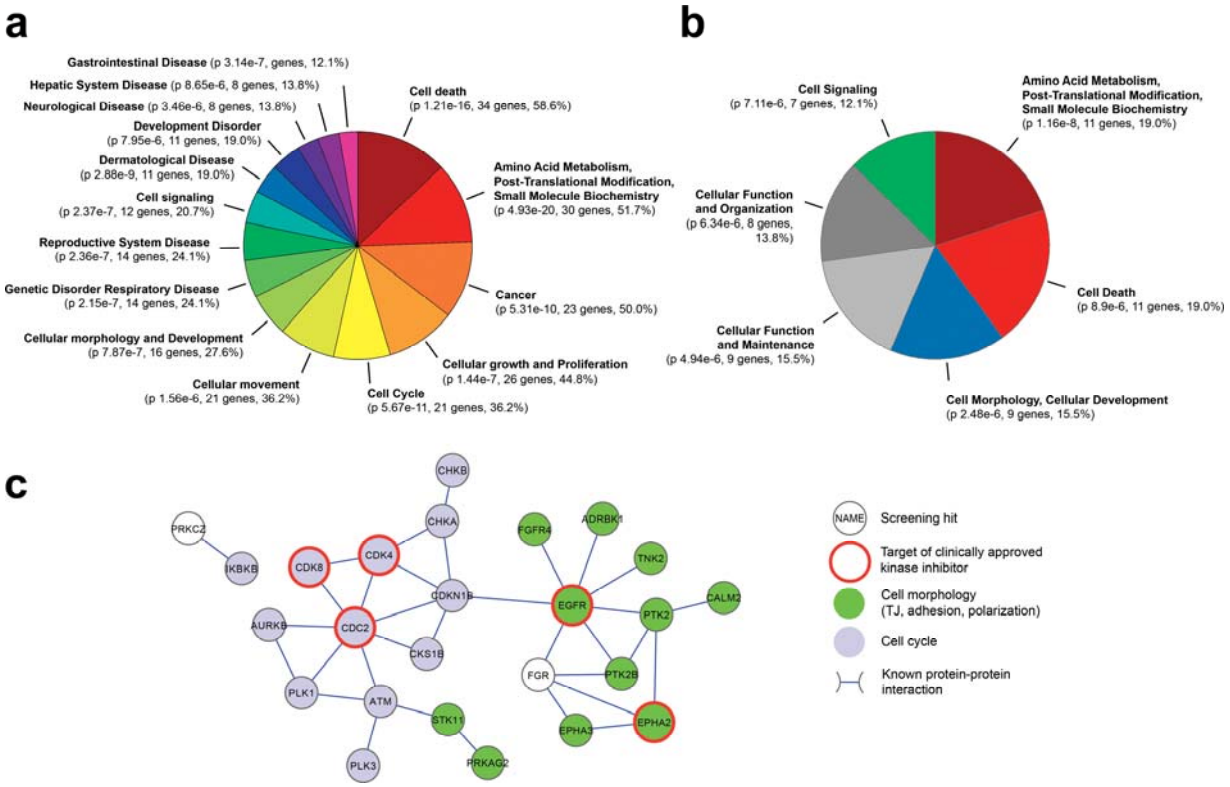

Supplementary Fig. 2. Biological process and protein association network analyses of the identified cellular kinases with marked impact on HCV entry. (**a**) The 58 identified cellular kinases involved in HCV entry and (**b**) the 18 identified kinases with impact on HCV but not on VSV entry were analyzed using the Ingenuity Pathways database. This analysis identified terms with the most prevalent biological processes associated with the identified candidate kinases within an organism (threshold $P<10^5$). The most significant terms of biological function were listed in the order of percentage frequency. (**c**) Protein association network of the 58 kinases involved in HCV entry identified by STRING analysis. Lines connecting kinases show direct (physical) and indirect (functional) associations derived from numerous sources, including experimental repositories, computational prediction methods and public text collections[6]. Kinases targeted by clinical licensed PKIs (red circles), kinases involved in the regulation of cell morphology including tight junctions, adhesion, cell polarity (green), cell cycle progression (blue) are highlighted.

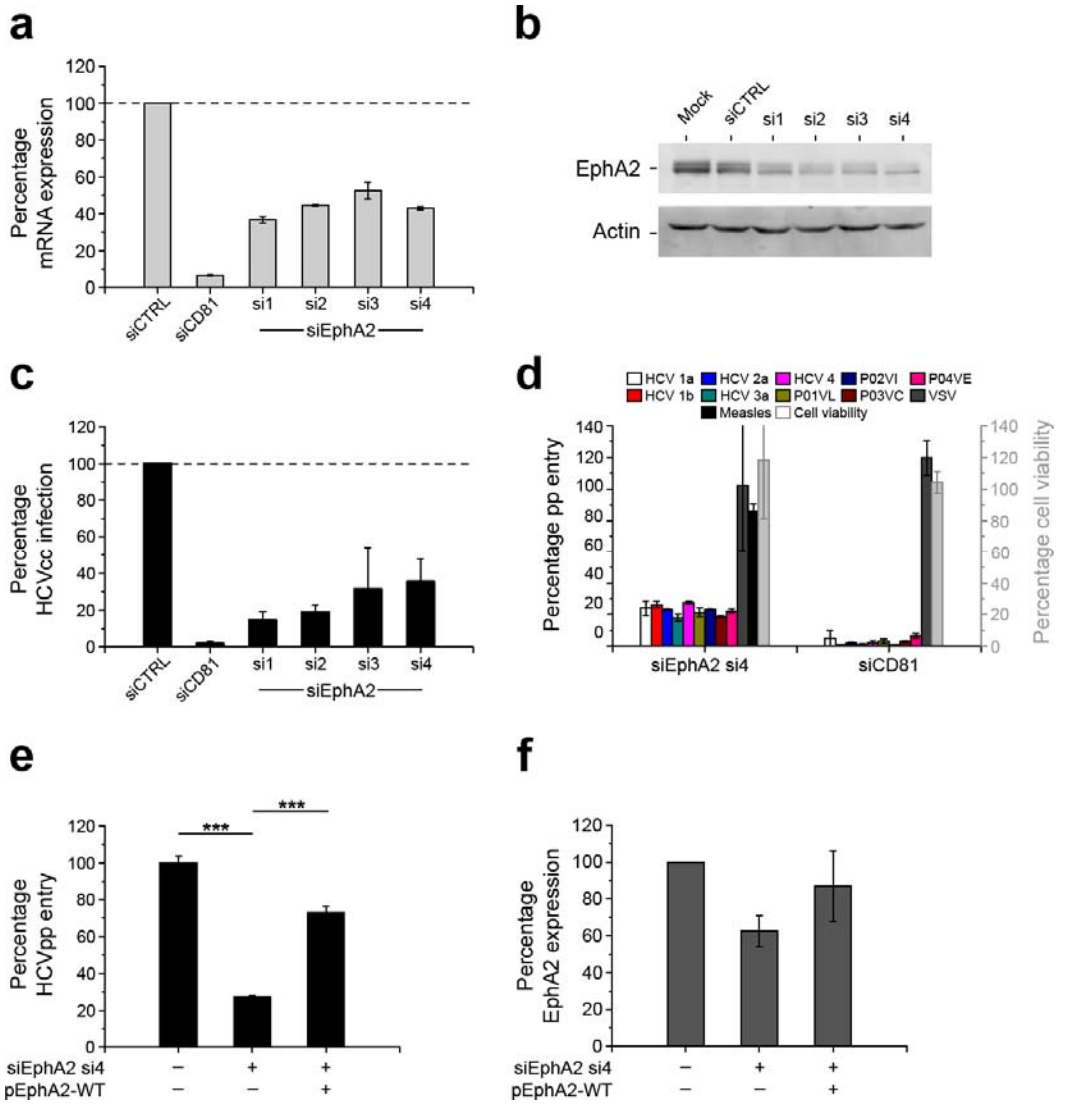

Supplementary Fig. 3. Ephrin receptor A2 (EphA2) is a co–factor for HCV entry. (a,b) Silencing of EphA2 expression in HCV permissive cells. **(a)** EphA2 mRNA (qRT–PCR analysis) and **(b)** protein expression (Western blot) in Huh7.5.1 cells transfected with EphA2–specific individual siRNAs (si1–si4). Silencing of CD81 mRNA expression by CD81–specific siRNA served as control. EphA2 mRNA (relative to GAPDH mRNA) and protein expression compared to cells transfected with control siRNA (siCTRL) is shown. **(c,d)** Inhibition of HCV infection and entry in cells with silenced EphA2 expression. **(c)** HCVcc infection in Huh7.5.1 cells transfected with individual siRNAs shown in panels **a,b**. siCTRL and CD81–specific siRNA served as internal controls. Data are expressed as percent HCVcc infection relative to siCTRL–transfected cells. **(d)** Entry of HCVpp containing envelope glycoproteins of various isolates in Huh7.5.1 cells transfected with siRNA si4. Analysis of VSV and measles virus pp entry or cells transfected with siCD81 served as controls. Data are expressed as percentage pp entry relative to siCTRL–transfected cells. **(d,e)** Rescue of HCV entry in cells with silenced EphA2 expression by exogenous EphA2. HCVpp entry **(e)** and EphA2 protein expression **(f)** in Huh7.5.1 cells co–transfected with EphA2–specific individual siRNA si4 and a cDNA encoding for siRNA si4–resistant EphA2 (pEphA2–WT)[51]. Protein expression was quantified using Image Quant analysis of Western blots. Data are expressed as percentage HCVpp entry relative to CTRL cells or as percentage EphA2 expression normalized for ß–actin expression. *** $P<0.0005$.

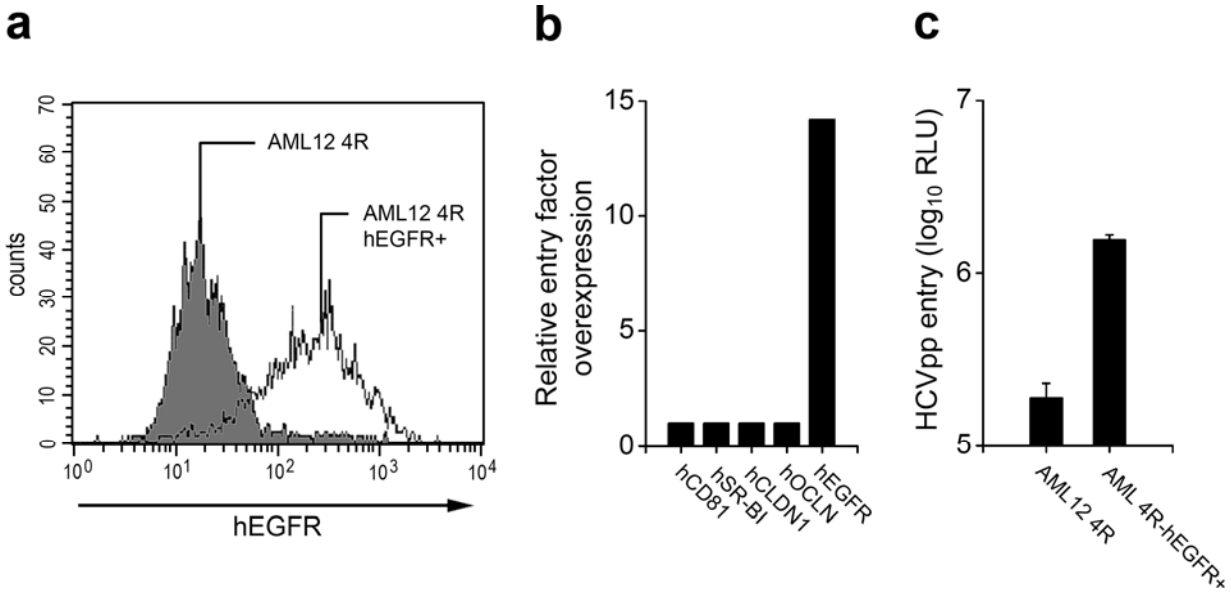

Supplementary Fig. 4. Expression of human EGFR enhances HCV entry into HCVpp permissive mouse hepatoma cells expressing human entry factors. Mouse hepatoma AML12 4R cells stably expressing human entry factors CD81, SR–BI, CLDN1, and OCLN were transduced with lentiviruses expressing human EGFR–L858R (hEGFR)[50]. Cell surface hEGFR expression (**a**) assessed by flow cytometry and (**b**) human CD81, SR–BI, CLDN1, OCLN and EGFR expression shown as fold expression relative to mock transduced AML12 4R cells. (**c**) HCVpp entry into mouse hepatoma cells engineered to express human EGFR. HCVpp entry was quantified in AML12 4R and AML12 4R–hEGFR+ cells in side–by–side experiments. Results are expressed as relative light units (RLU).

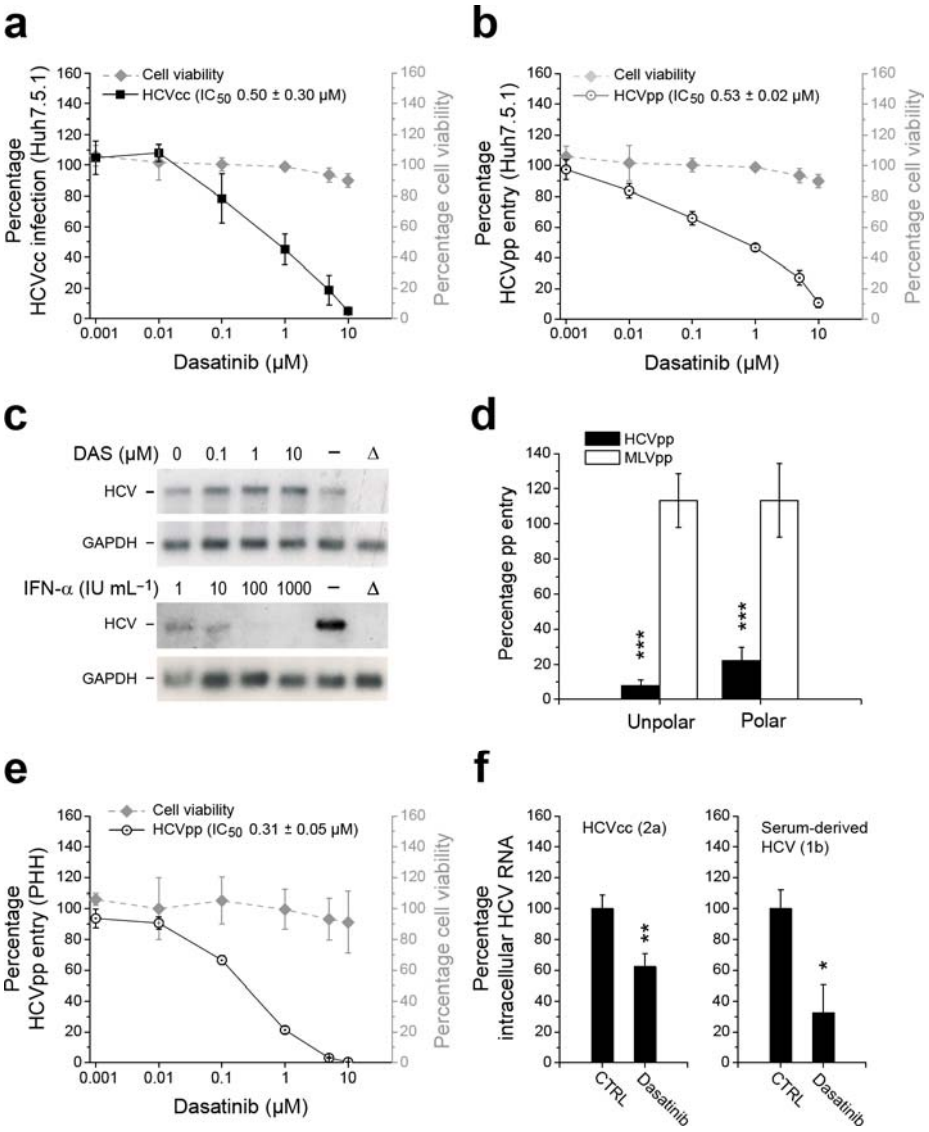

Supplementary Fig. 5. Dose–dependent inhibition of HCV entry and infection by *Dasatinib* – a clinically approved inhibitor of EphA2 kinase. (**a,b**) Effect of *Dasatinib* on HCVpp entry and HCVcc infection. (**a**) HCVcc infection and (**b**) HCVpp entry in *Dasatinib*– or CTRL–treated Huh7.5.1 cells was assessed as described[27,40]. Cell viability was assessed using MTT assay. IC_{50} values are expressed as median of three independent experiments ± standard error of the median. (**c**) Effect of *Dasatinib* on HCV replication. Following electroporation with HCV RNA from the subgenomic HCV JFH1 replicon or replication incompetent HCV RNA (GND, Δ) Huh7.5 cells were incubated with solvent CTRL, *Dasatinib,* or interferon–α (IFN–α–2a) at the indicated concentrations. HCV RNA and GAPDH mRNA were analyzed by Northern blot. (**d**) Effect of *Dasatinib* on HCVpp entry into polarized HepG2–CD81 cells. HCVpp and MLVpp entry was analyzed in non–polarized and polarized HepG2–CD81 cells pre–incubated with *Dasatinib* (means ± SEM). (**e**) Effect of *Dasatinib* on HCVpp entry into PHH. HCVpp entry was assessed in PHH pre–treated with *Dasatinib*. Viability of treated cells was assessed using MTT assay. IC_{50} values are expressed as median of three independent experiments ± standard error of the median. (**f**) Effect of *Dasatinib* on HCV infection of PHH. Intracellular HCV RNA in PHH infected with HCVcc[59] or serum–derived HCV[40] in *Dasatinib* or solvent CTRL–treated PHH was analyzed by qRT–PCR[40]. Cell viability was assessed using MTT assay. *, $P<0.05$, **, $P<0.005$; ***, $P<0.0005$. Unless otherwise indicated: *Dasatinib* 10 µM.

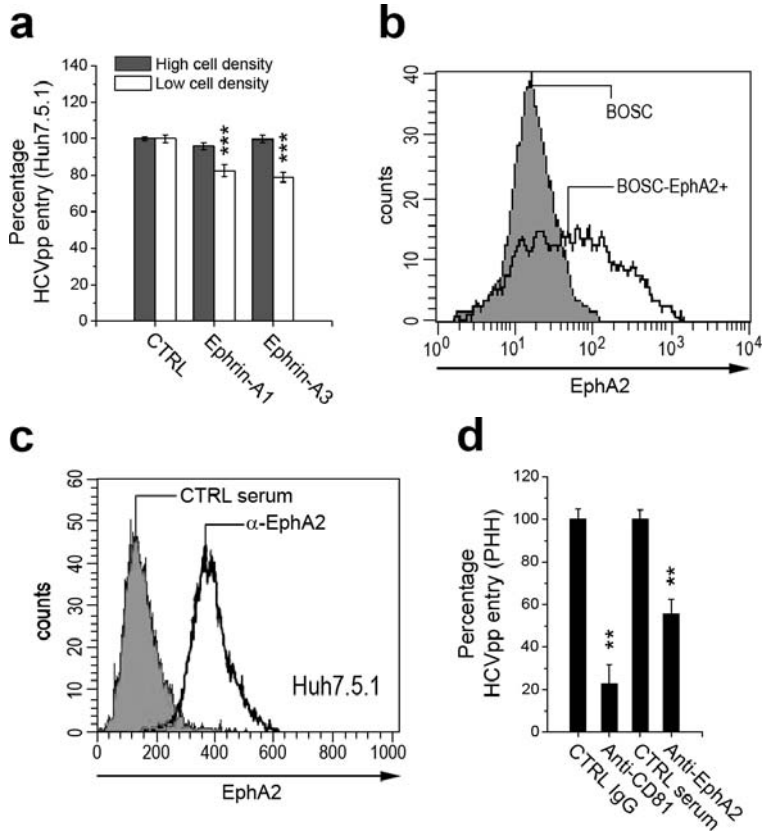

Supplementary Fig. 6. EphA2–specific ligands and antibodies modulate HCV entry. (**a**) Effect of EphA2–specific ligands ephrin–A1 and –A3 and cell–density on HCVpp entry. HCVpp entry into cells seeded at high or low density treated with 1 μg mL^{-1} soluble Fc–tagged ephrin–A1 and –A3 or Fc–tag (CTRL)[64] is shown. (**b**) Specific binding of rat serum to human EphA2 (dilution 1:5,000) to cell surface human EphA2 expressed on BOSC cells. Flow cytometric analysis of BOSC cells transfected with a human EphA2 expression construct (non shaded histograms; "BOSC–EphA2+") or a an empty control vector (pcDNA3; "BOSC", grey histograms)[54]. (**c**) Specific binding of EphA2–specific serum (dilution 1:100) to native EphA2 expressed on the surface of Huh7.5.1 cells. Flow cytometric analysis of non–permeabilized Huh7.5.1 cells incubated with EphA2–specific (non shaded histograms) or control serum (grey histograms) is shown. (**d**) Effect of EphA2–specific serum on HCVpp entry into PHH. HCVpp entry into PHH in the presence or absence of antibody to CD81 (10 μg mL^{-1}) or serum to EphA2 (dilution 1:50) is shown. **, $P<0.005$; ***, $P<0.0005$.

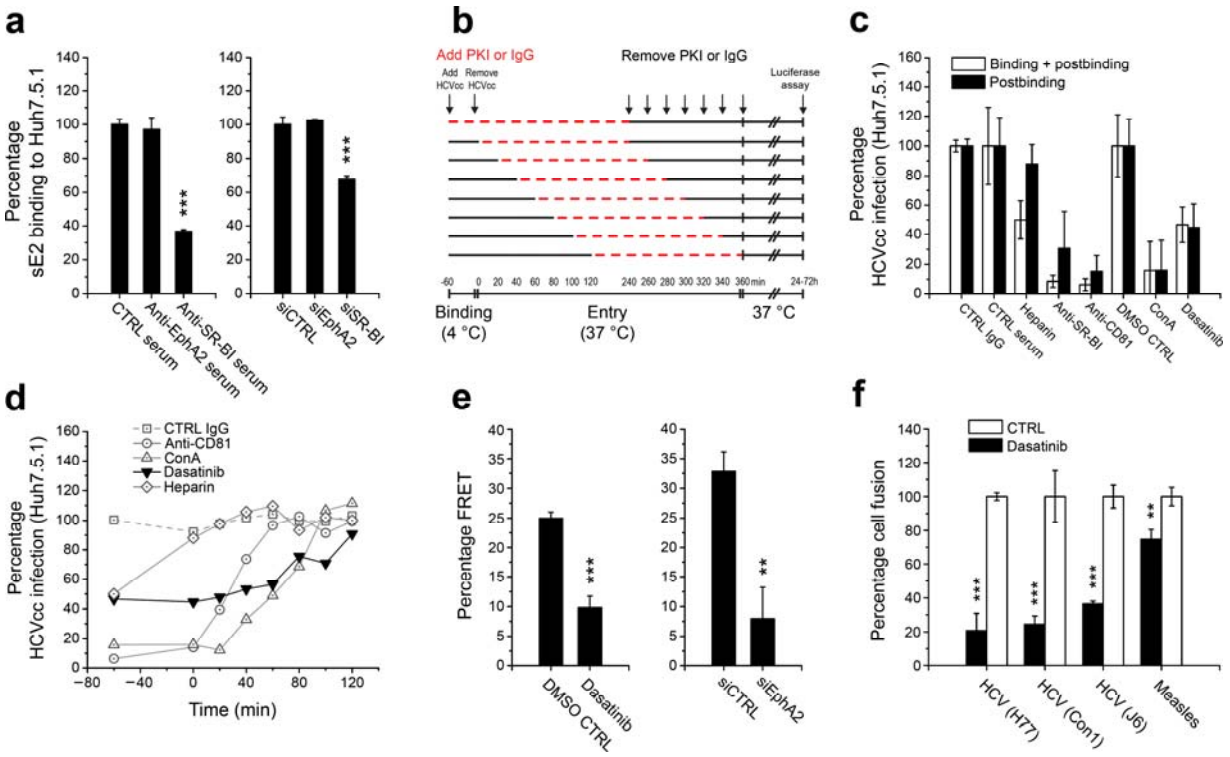

Supplementary Fig. 7. EphA2 mediates entry at a postbinding step by promoting the formation of CD81–CLDN1 co–receptor association(s). (**a**) EphA2 and binding of soluble HCV glycoprotein sE2 to HCV permissive cells. sE2 binding to Huh7.5.1 cells incubated with EphA2–specific serum or siEphA2 were analyzed by flow cytometry. SR–BI–specific antibodies and SR–BI silencing served as positive controls (all antibodies diluted at 1:100). (**b,c**) Effect of *Dasatinib* on HCV binding and postbinding steps. (**b**) Experimental setup. After HCVcc binding to Huh7.5.1 cells for 1 h at 4 °C in the presence or absence of antibodies, where HCVcc bind to the cells but do not efficiently enter, the inoculum is removed and the cells are shifted to 37 °C to allow synchronous viral entry[48,54,62,63]. Dashed lines indicate the presence of compounds. Data are expressed relative to HCVcc infection without compound. (**c**) To discriminate between virus binding and postbinding events, HCVcc binding to Huh7.5.1 cells was performed in the presence or absence of indicated compounds at 4 °C, before cells were washed and incubated with compounds at 37 °C. (**d**) HCV entry kinetics. Time–course of HCVcc infection of Huh7.5.1 cells following addition of the indicated compounds at different time–points during infection (**Supplementary Methods**). (**e**) Effect of *Dasatinib* and EphA2 silencing on CD81–CLDN1 association(s). FRET of CD81–CLDN1 co–receptor associations in HepG2–CD81 cells incubated with *Dasatinib* or EphA2–specific siRNA are shown (means ± SEM). (**f**) Effect of *Dasatinib* on membrane fusion. Viral glycoprotein–dependent fusion of 293T cells with Huh7 cells pre–incubated with *Dasatinib* or control is shown. **, $P<0.005$; ***, $P<0.0005$. *Dasatinib:* 10 µM.

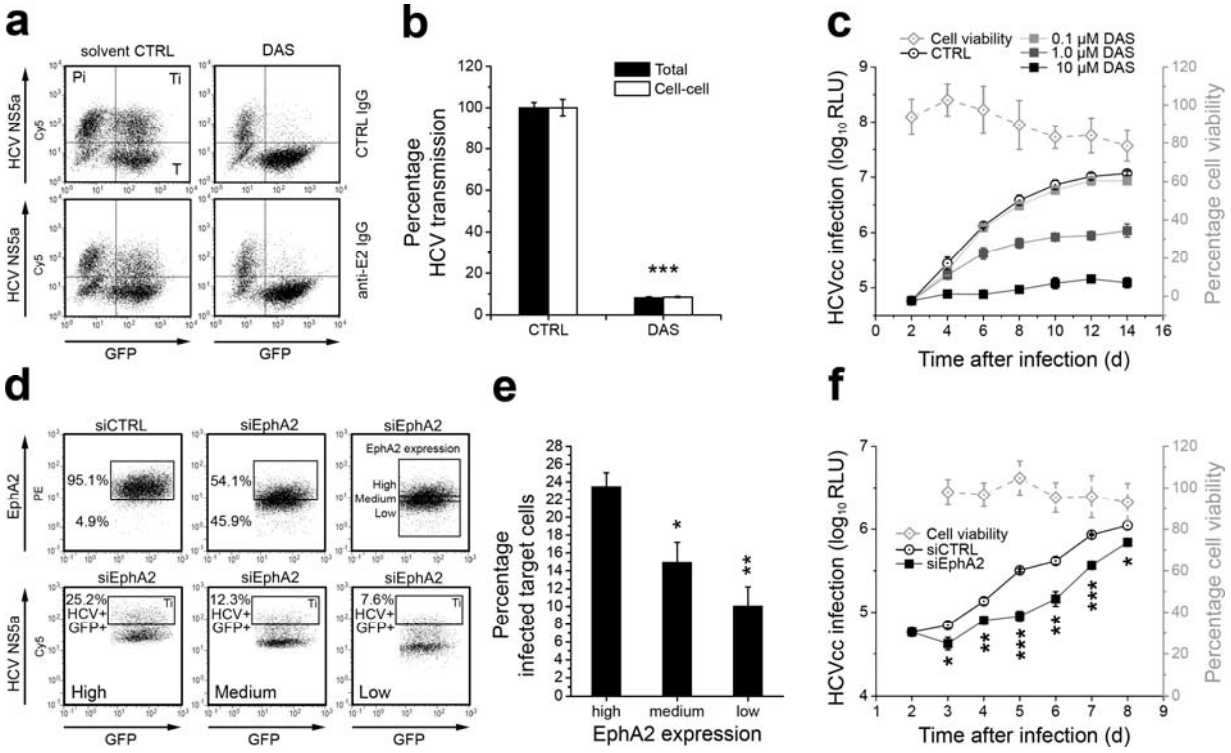

Supplementary Fig. 8. EphA2 plays a functional role in HCV cell–cell transmission and spread. The experimental set–up of the HCV cell–cell transmission assay is described in **Fig. 5**. (**a**) Relative quantification of HCV–infected target cells (Ti) after co–cultivation with HCV producer cells (Pi) during *Dasatinib* treatment in the absence (cell–free and cell–cell transmission) and presence (cell–cell transmission) of HCV E2–specific antibody. (**b**) Total and cell–cell transmission were defined as HCV infection of Huh7.5–GFP+ target cells (Ti) in the absence (total transmission, black bars) or presence (cell–cell transmission, white bars) of HCV E2–specific antibody. (**c**) Effect of *Dasatinib* on viral spread. Long–term HCVcc infection of Huh7.5.1 cells incubated with *Dasatinib* 48 h post–infection at the indicated concentrations. Medium with solvent (CTRL) or PKI was replenished every 2nd day. Cell viability was assessed using MTT test. (**d**) EphA2 expression in target cells with silenced EphA2 expression. Cell surface EphA2 expression was analyzed by flow cytometry and target cells were divided in three groups displaying high, medium and low EphA2 expression. (**e**) Cell–cell transmission in HCV–infected GFP+ target cells with high, medium and low EphA2 expression was quantified by flow cytometry as described in **Fig. 5**. (**f**) Effect of EphA2 silencing on viral spread. Long–term analysis of HCVcc infection in Huh7.5.1 transfected with EphA2–specific or control siRNA 24 h post–infection. Cell viability was assessed using MTT test. DAS= *Dasatinib* 10 µM (unless otherwise stated). *, $P<0.05$; **, $P<0.005$; ***, $P<0.0005$.

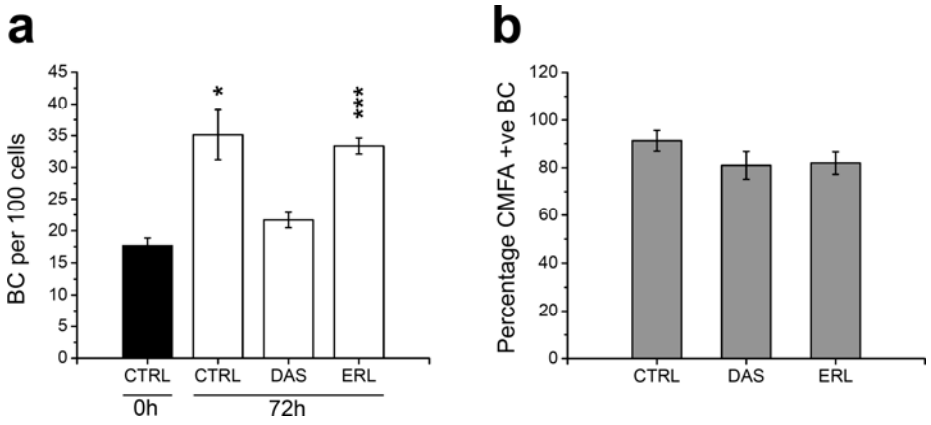

Supplementary Fig. 9. Effect of PKIs on polarization and tight junction integrity of HCV permissive HepG2–CD81 cells. (**a**) Polarity in HepG2–CD81 cells incubated with PKIs. HepG2–CD81 cells were incubated in the presence of *Erlotinib* or *Dasatinib* for 72 h, fixed in 3% paraformaldehyde and stained for bile canaliculi (BC) that expressed marker MRP2. The polarity index (BC per 100 cells) was assessed by quantifying the number of MRP2 positive BC per 100 cell nuclei for five fields of view on 3 replicate cover slips. (**b**) Tight junction (TJ) integrity in HepG2–CD81 cells incubated with PKIs. TJ integrity was assessed after 72 h PKI treatment by determining the frequency of BC retaining marker dye CMFDA as described previously[18]. Means ± SEM are shown. *, $P<0.05$; ***, $P<0.0005$. PKI: 10 μM, DAS= *Dasatinib*, ERL= *Erlotinib*.

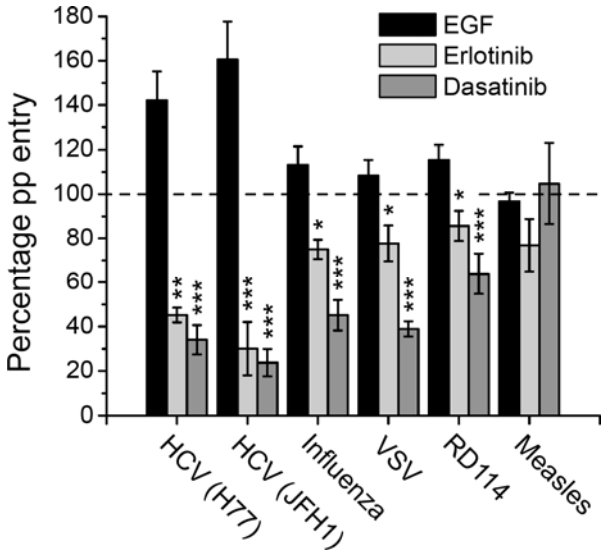

Supplementary Fig. 10. Effect of EGF and PKIs on entry of pseudoviruses expressing envelope proteins from HCV, VSV, influenza, measles and feline leukemia virus. Infection of serum–starved Huh7.5 cells incubated with EGF (1 μg mL^{-1}) or PKI (10 μM) with pseudotyped particles expressing envelope glycoproteins from HCV strains H77 and JFH1, influenza, vesicular stomatitis virus (VSV), endogenous feline leukemia virus (RD114) and measles virus. *, $P<0.05$; **, $P<0.005$; ***, $P<0.0005$.

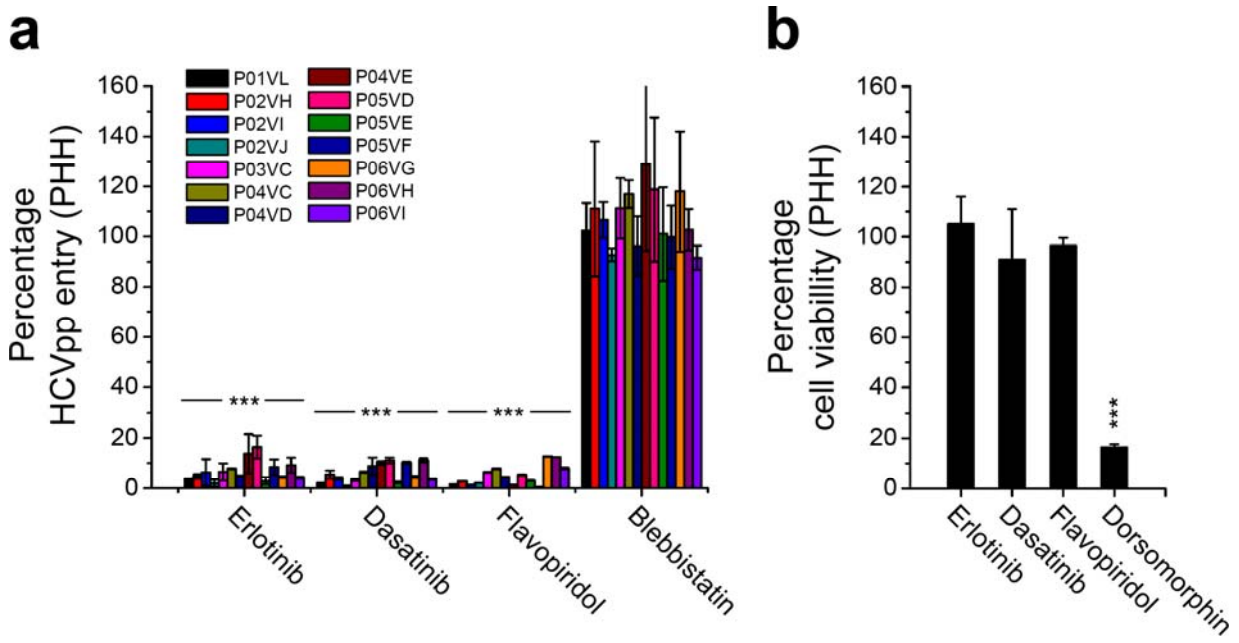

Supplementary Fig. 11. *Erlotinib, Dasatinib,* and *Flavopiridol* inhibit entry of HCV escape variants which are resistant to autologous host immune responses. HIV–based HCVpp bearing envelope glycoproteins from HCV escape variants P01VL, P02VH, P02VI, P02VJ, P03VC, P04VC, P04VD, P04VE, P05VD, P05VE, P05VF, P06VG, P06VH, P06VI isolated during liver transplantation from six different HCV–infected patients[27] were produced as described (**Supplementary Methods**)[27]. (**a**) Effect of *Dasatinib*, *Erlotinib,* or *Flavopiridol* on entry of HCV escape variants. HCVpp entry into PHH pre-incubated with PKIs (10 μM) is shown. Incubation of cells with *Blebbistatin* (10 μM) served as negative control. (**b**) Analysis of cell viability in PKI–treated cells. Cell viability was assessed by MTT assay. Incubation with *Dorsomorphin* (10 μM), an unrelated PKI, served as positive control for cell viability. ***, $P<0.0005$.

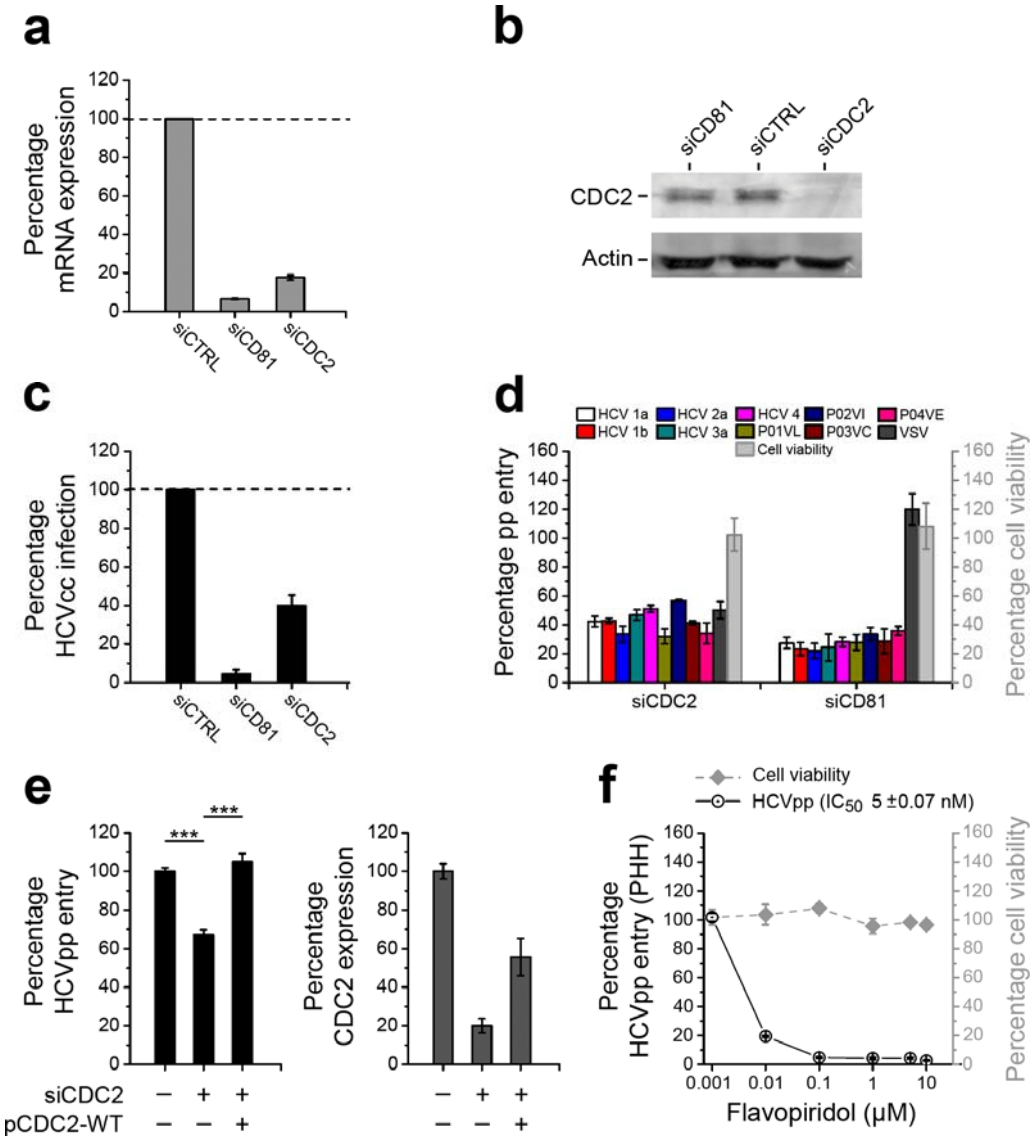

Supplementary Fig. 12. Cell division cycle 2 kinase (CDC2) is a co–factor for HCV entry. (**a**) Silencing of CDC2 expression in HCV permissive cells. **(a)** CDC2 mRNA (quantification by qRT–PCR relative to GAPDH mRNA) and (**b**) protein expression (Western blot) in Huh7.5.1 cells transfected with an individual CDC2–specific siRNA compared to control siRNA (siCTRL) is shown. Silencing of CD81 expression by CD81–specific siRNA served as control. (**c**) HCVcc infection in Huh7.5.1 cells with silenced CDC2 expression (as shown in panels **a,b**). (**d**) Entry of HCVpp containing envelope glycoproteins of various isolates[27,65] in Huh7.5.1 cells with silenced CDC2 expression (as shown in panels **a,b**). Data are expressed as percent pp entry relative to siCTRL–transfected cells. Cell viability in siCDC2–treated cells assessed using MTT test is shown as mean ± SEM. (**e**) Rescue of HCV entry in cells with silenced CDC2 expression by exogenous CDC2. HCVpp entry and CDC2 protein expression in Huh7.5.1 cells co–transfected with CDC2–specific siRNA and cDNA encoding for RNAi–resistant CDC2 is shown. Different transfection protocols (poly–cationic transfection (**a–d)** versus electroporation (**e**) are responsible for the apparent differences in Hs–CDC2_14–siRNA efficacy on reducing HCVpp entry. Protein expression was quantified using Image Quant analysis of Western blots. Data are expressed as percentage HCVpp entry relative to CTRL cells or as percentage CDC2 expression normalized for ß–actin expression (means ± SEM). *** $P<0.0005$. (**f**) Effect of *Flavopririol*, a CDC2–inhibitor, on HCVpp entry into PHH. Cell viability was assessed using MTT assay.